Effect of ISA and chloride on the uptake of niobium (V) by hardened cement paste and C-S-H phases: Quantitative description and mechanistic understanding

Yongheum Jo [a,1,*], Neşe Çevirim-Papaioannou [a], Karsten Franke [b], Markus Fuss [a], Malene Pedersen [c], Barbara Lothenbach [c], Benny de Blochouse [d], Marcus Altmaier [a], Xavier Gaona [a,**]

[a] Institute for Nuclear Waste Disposal, Karlsruhe Institute of Technology, Karlsruhe, Germany
[b] Institute of Resource Ecology / Institute of Radiopharmaceutical Cancer Research, Helmholtz-Zentrum Dresden-Rossendorf (HZDR), Research Site Leipzig, Germany
[c] Laboratory Concrete & Asphalt, Empa, Swiss Federal Laboratories for Materials Science and Technology, Dübendorf, Switzerland
[d] ONDRAF/NIRAS, Sint-Joost-ten-Node, Belgium

ARTICLE INFO

Keywords:
Niobium
Hardened cement paste (HCP)
Limestone
Calcium silicate hydrate (C-S-H) phases
Sorption

ABSTRACT

The uptake of niobium by hardened cement paste (HCP) and calcium silicate hydrate (C-S-H) phases was investigated with ^{93}Nb and ^{95}Nb ($t_{1/2}$ 35.0 days). Structural materials used in nuclear reactors as well as cements contain the naturally occurring isotope ^{93}Nb, while radioactive ^{94}Nb with $t_{1/2}$ 2×10^4 years is relevant in the context of nuclear waste disposal. Strong uptake of Nb was observed for both materials, confirming that C-S-H is the main sink of Nb in cement. Isotopic exchange with ^{93}Nb in cement can play a role in the uptake of ^{94}Nb under repository conditions. The formation of complexes with isosaccharinic acid (ISA) decreases the Nb uptake, although sorption remains strong up to $[ISA]_{tot}$ 0.1 M. Chloride has a negligible effect on the uptake of Nb up to [NaCl] 2 M. This work provides a sound basis for the quantitative description and mechanistic understanding of ^{94}Nb retention in L/ILW repositories.

1. Introduction

Niobium (Nb) is present in the earth's crust with an abundance of ca. 20 ppm. Among many other applications, Nb is widely used in the manufacture of various alloys. Structural materials such as stainless steel and Ni-based alloys used in nuclear reactors contain the naturally occurring and inactive isotope ^{93}Nb [1]. During the operation of nuclear power plants, neutron activation of ^{93}Nb (i.e., $^{93}Nb + n \rightarrow {}^{94}Nb +$ gamma-ray) produces the long-lived isotope ^{94}Nb ($t_{1/2} = 20{,}000$ a), which is accumulated during the residence time in the reactor. Specific waste streams resulting from the dismantling of nuclear reactors containing ^{94}Nb will be disposed in repositories for low- and intermediate-level radioactive waste (L/ILW) [2,3], in which this radionuclide has been potentially identified as one of the relevant contributors to the effective dose [4,5].

Cementitious materials (e.g., concrete, shotcrete, grout) are ubiquitous in most disposal concepts for nuclear wastes, mainly for construction purposes and for the sealing of the excavated tunnels [6,7]. In L/ILW repositories, cementitious materials are extensively used as waste packages, overpacks, backfill, as well as for the solidification and stabilization of the waste [8]. Upon contact with groundwater, cementitious materials undergo degradation following three main stages [9–11]. The first degradation stage of cement involves the dissolution of alkali (hydr-)oxides, resulting in high concentrations sodium and potassium in the pore water ([Na] + [K] ≈ 0.3–0.5 M) as well as hyperalkaline conditions i.e., pH ≈ 13–13.5. The porewater composition in the second degradation stage is buffered by the dissolution of portlandite, $Ca(OH)_2$, resulting in pH ≈ 12.5 and [Ca] ≈ 0.02 M. The third degradation stage is dominated by the incongruent dissolution of calcium silicate hydrate (C-S-H) phases. Within degradation stage III, the Ca:Si ratio (C:S) of the C-S-H phases varies from ≈ 1.6 to ≈ 0.6, resulting in a drop in pH from ≈ 12.5 to ≈ 10 [12,13]. Calcite ($CaCO_3$) is often

* Correspondence to: Y. Jo, Department of Nuclear Engineering, Hanyang University, Seoul, Republic of Korea.
** Corresponding author.
E-mail addresses: yongheumjo@hanyang.ac.kr (Y. Jo), xavier.gaona@kit.edu (X. Gaona).
[1] Current address: Department of Nuclear Engineering, Hanyang University, Seoul, Republic of Korea.

considered as the main phase remaining after the complete degradation of cement [10].

Large inventories of cellulose are disposed of with the waste in most repositories for L/ILW. Isosaccharinic acid (ISA) is the main degradation product of cellulose in the hyperalkaline conditions defined by cementitious environments. ISA has been shown to form strong complexes with hard Lewis acids under alkaline conditions, e.g., with Th(IV) [14–16], Pu(III/IV) [17–19], Zr(IV) [20], Am(III) [15], Ni(II) [21], among others. The formation of such complexes can importantly affect solubility phenomena and sorption processes of these radionuclides in cementitious systems, and thus deserves a close inspection in the context of repositories for L/ILW. High concentrations of chloride (up to ≈ 4–5 M) have been described for specific waste streams containing evaporator concentrates (from nuclear power plants operation) [2]. These high chloride concentrations can affect the retention of radionuclides in cementitious environments by altering the speciation of the radionuclides in the aqueous phase, modifying the chemistry of cement (surface properties, cement phases), or both.

Cementitious materials play a relevant role in the retention of radionuclides and thus are considered as part of the multi-barrier system in different repository concepts [10,22]. In particular, C-S-H phases have been described to be the main sink for actinides (An) [23,24], lanthanides (Ln) [25] and several transition metals of relevance for nuclear waste disposal, e.g., Ni [26], Tc [27], etc. A few studies have investigated the uptake of Nb by cementitious materials, although discrepant distribution coefficients (R_d) are reported in the literature for this system and the retention mechanism remains ill-defined. Pilkington and Stone investigated the uptake of ^{93}Nb by mixtures of 10:1 Pulverised Fuel Ash / Ordinary Portland Cement at pH = 11.8 and [Ca] = 9.2×10^{-4} M [28]. A large dispersion in the distribution coefficients was observed ($R_d = 5 \times 10^2$–8×10^4 L·kg^{-1}). Sorption experiments were performed at largely oversaturated conditions (initial niobium concentration, $C_0 = 5.3 \times 10^{-3}$ M), where secondary Nb solid phases or colloids are expected to form. Baker and coworkers performed sorption experiments with active ^{95}Nb ($t_{1/2}$ = 35.0 days) and a cement-based Nirex Reference Vault Backfill in 0.5 M NaCl solutions [29]. A strong sorption was reported by the authors, with R_d values ranging from 3.5×10^4 to 4.1×10^4 L·kg^{-1}. Pointeau et al. investigated the sorption of ^{95}Nb by degraded hardened cement pastes (CEM I and CEM V) and C-S-H phases with Ca:Si ratios (C:S) of 0.7, 1.0, and 1.3. HCP and C-S-H phases with a higher C:S showed a slightly stronger sorption ($R_d = 1 \times 10^5$–2×10^5 L·kg^{-1}), compared to C-S-H phases with lower C:S ratios ($R_d = 4 \times 10^4$–7×10^4 L·kg^{-1}) [30]. Wieland reviewed the sorption data available for Nb(V) and selected a conservative estimate (R_d = 1000 L·kg^{-1}) accounting for the ill-defined aqueous speciation of Nb(V) in hyperalkaline systems [22]. The reference book by Ochs, Mallants, and Wang selected $R_d = 5 \times 10^4$ L·kg^{-1} as best estimate for the uptake of Nb(V) by HCP in the degradation stages I–III, with upper and lower limits defined as 1×10^6 and 1×10^3 L·kg^{-1}, respectively. The selection was based on the available data for Nb(V), but also in analogy with Sn(IV), which is expected to display similar predominant anionic hydrolysis species in hyperalkaline conditions, i.e., $Sn(OH)_6^{2-}$ and $Nb(OH)_7^{2-}$ [10]. However, we note that recent studies have provided evidence on the formation of ternary complexes Ca–Nb(V)–OH in aqueous systems representative of cementitious environments, although the precise stoichiometry and thermodynamic properties of these complexes remain unknown [31,32].

In our previous study, we investigated the uptake of ^{95}Nb(V) by HCP CEM I in the degradation stage I (pH ≈ 13.5) in the absence and presence of ISA and chloride [33]. In the absence of ISA, sorption experiments revealed a fast (steady state attained at t ≈ 2 days) and strong uptake with 5 ≤ log R_d (in L·kg^{-1}) ≤ 7. The chemical analysis of the pristine HCP revealed a considerable content of inactive ^{93}Nb (3.1 ± 0.3 ppm), thus suggesting (for the first time) that isotopic exchange might be a relevant retention mechanism for other Nb isotopes (e.g., ^{95}Nb in the experiments or ^{94}Nb in the waste). ISA was found to decrease the retention of Nb(V) by HCP at [ISA] > 10^{-3} M, although sorption remained moderately strong, with log R_d (in L·kg^{-1}) ≈ 3.5 at [ISA] ≈ 0.1 M. This effect was explained by the possible formation of stable (Ca–)Nb(V)–ISA complexes in the aqueous phase, although the stoichiometry and thermodynamic stability of these complexes was not determined. Similar observations have been reported for the uptake of An(III)/Ln(III) and An(IV) by HCP in the presence of ISA [9,22,34]. The chloride effect on the uptake was evaluated to be minor.

In this context, the present work investigates the uptake of Nb(V) by HCP in the degradation stage I, and the effect of ISA and chloride on the retention process. The study focuses on a CEM III/C (Portland cement blended with >80 wt% of blast furnace slag) with and without the addition of limestone ($CaCO_3$), thus complementing and further extending our previous work with CEM I [33]. These materials are considered for the construction of near-surface repositories for the disposal of L/ILW [35]. Besides the quantitative evaluation of the uptake process, this study further explores the mechanism/s driving the uptake of niobium by cementitious materials. For this purpose and in addition to isotope exchange with ^{93}Nb(V) in pristine cement, the uptake of Nb (V) by C-S-H phases is investigated with a series of sorption experiments where total niobium concentration (as [^{95}Nb + ^{93}Nb]) is varied over seven orders of magnitude. The possible role of Nb(V) solubility phenomena is discussed in connection with our previous study dedicated to the identification of the Ca–Nb(V)–OH solid phases controlling the solubility of Nb(V) in cementitious systems [32].

2. Experimental

2.1. Chemicals and materials

NaCl (EMSURE®), KCl (EMSURE®), NaOH (Titrisol®), KOH (Titrisol®), Na_2SO_4 (EMSURE®), $CaCO_3$ (EMSURE®), $Ca(OH)_2$ (EMSURE®), HCl fuming 37 % (EMSURE®), 48 % HF (Ultrapur), 31 % H_2O_2 (Ultrapur), and 30 % HCl (Ultrapur) were obtained from Merck. KOH pellets (99.98 % metal grade) and $NbCl_5$ (99 %) were purchased from Alfa Aesar and Sigma-Aldrich, respectively. Suprapur (65 %) and Ultrapur (60 %) HNO_3 obtained from Merck were used for the dilution of samples for inductively coupled plasma atomic emission spectroscopy (ICP-OES) and inductively coupled plasma-mass spectrometry (ICP-MS), respectively.

Isosaccharinic acid-1,4-lactone was obtained from Biosynth Carbosynth and Interchim. The results of elemental analysis, non-purgeable organic carbon (NPOC), ion chromatography (IC) and ^{1}H NMR confirmed the purity of the commercial products (see Fig. SI-1 in the Supporting Information). A stock solution of ISA was prepared by dissolving ISA lactone in 1 M KOH + 1 M NaOH solutions. The concentration of the stock solution was determined as [ISA] = 1.15 M by NPOC and IC.

All samples were prepared in Ar-glove boxes (MBRAUN) with $O_2 < 1$ ppm at $T = (22 \pm 2)$ °C. All solutions were prepared using purified water (Milli-Q academic, Millopore, 18.2 MΩ·cm), purged with Ar for >2 h, and equilibrated overnight in the glovebox before use in order to remove dissolved CO_2(g). Measurements of pH were performed using combination pH electrodes (ROSS Orion) and calibrated against commercial buffer solutions (pH = 10–13, Merck).

2.2. Preparation active Nb stock solutions

Two sources of active Nb isotopes were used in the present study: active Nb isotopes (mixture of ^{91m}Nb, ^{92m}Nb, ^{95}Nb and ^{95m}Nb) obtained from the irradiation of a ^{nat}Zr foil in a cyclotron (Section 2.2.1), and a ^{95}Nb stock resulting from the decay of a commercially available (aged) ^{95}Zr (Section 2.2.2).

2.2.1. ^{95}Nb stock solution obtained from irradiation of a ^{nat}Zr foil

The (d,x) nuclear reaction on a zirconium target was used to produce

active Nb isotopes. A Zr foil (0.12 mm thick, 99.5 % purity, Alfa Aesar) with the natural isotopic abundance was bombarded by 9 MeV deuterons with 700 μAh for 73 h using the COSTIS target station (IBA RadioPharma Solutions, Belgium) placed at a beam line at port 3 of the cyclotron Cyclone 18/9® (IBA RadioPharma Solutions, Belgium) at the research facility HZDR (Helmholtz-Zentrum Dresden-Rossendorf), Leipzig. After the irradiation, the target was stored for ca. 6 days in order to decrease the presence of undesired short-lived radionuclides. The irradiated Zr foil was dissolved in 48 % HF, and the separation of the Nb isotopes from the bulk Zr was performed using a combination of ion-exchange resins (DOWEX® 50 X8 and UTEVA). The separation process was developed on the basis of previously reported methods [33,36,37]. A detailed description of the modified method is provided in the section 1.2 of the Supporting Information.

The active Nb and Zr isotopes remaining in the solution after filtration were quantified by gamma spectrometry. A high purity germanium detector (61 mm × 46 mm, Mirion) was used for the measurement, and the detector was calibrated using multi-element standard solutions (Eckert & Ziegler) in the energy range of 45–1800 keV. The energy resolution was 1.8 keV at 1.33 MeV and 0.875 keV at 122 keV. The sample geometry was defined with 10 mL PP narrow neck vial (Kautex). The activities of ^{91m}Nb ($t_{1/2}$ = 65.0 d), ^{92m}Nb ($t_{1/2}$ = 10.2 d), ^{95}Nb ($t_{1/2}$ = 35.0 d), and ^{95}Zr ($t_{1/2}$ = 64.0 d) were quantified by the gamma lines at 1205.0 keV, 1205.0 keV, 934.5 keV, 765.8 keV, and 756.7 keV, respectively. The activity of the stock solution measured after separation was considered as the reference activity at t = 0, which was used for the correction of the decay in the course of the sorption experiments. At t = 0, the concentration and activities of the Nb and Zr isotopes were determined as: [^{91m}Nb] = (3.1 ± 0.1) × 10^{-9} M (0.23 ± 0.01 MBq·mL^{-1}), [^{92m}Nb] = (9.9 ± 0.1) × 10^{-10} M (0.47 ± 0.02 MBq·mL^{-1}), [^{95}Nb] = (1.4 ± 0.1) × 10^{-9} M (0.20 ± 0.01 MBq·mL^{-1}), and [^{95}Zr] < 6.6 × 10^{-12} M (< 0.5 kBq·mL^{-1}, detection limit of gamma spectrometry in the stock condition with high activity from Nb isotopes). Because of the probability of the gamma transitions considered for the detection of the Nb isotopes, the quantification of niobium was achieved via ^{95}Nb. The presence of other active isotopes of niobium besides ^{95}Nb is not discussed further in the following sections.

The concentrations of inactive Nb and Zr isotopes were measured by ICP-MS, resulting in [^{93}Nb] = 1.60 × 10^{-7} M and [Zr] < 3.6 × 10^{-8} M (detection limit of ICP-MS). Due to the short half-life of the Nb isotopes (i.e., $t_{1/2}$ = 35.0 d for ^{95}Nb), sorption experiments were conducted within 40 days after completing the separation process. This stock solution was primarily used for sorption experiments with HCP.

2.2.2. *^{95}Nb stock solution obtained from the decay of a commercial ^{95}Zr solution*

A commercial ^{95}Zr stock solution (7.4 MBq, in 0.5 M oxalic acid) was obtained from Eckert & Ziegler. At the time of reception at KIT-INE (t = 0), the ^{95}Zr stock solution was more than one year old with the result of a significant in-growth of ^{95}Nb being present as main decay product of ^{95}Zr. The activity of ^{95}Nb at t = 0 was quantified as 8.7 MBq. The concentrations of inactive isotopes of Nb and Zr in this stock solution were also determined by ICP-MS, resulting in [^{93}Nb] = 4.5 × 10^{-7} M and [^{94}Zr] = 7.0 × 10^{-3} M. The effect of Zr on R_d values for Nb sorption was negligible (see Fig. SI-3 in the Supporting Information). No impact of oxalic acid on the sorption of Nb is expected due to the low initial concentration of the ligand in the sorption samples ([oxalate]$_0$ ≈ 1 × 10^{-4} M, considering spikes of 3.6 kBq ^{95}Nb per sample) and the further decrease in the concentration due to the precipitation of the sparingly soluble Ca(ox)·xH$_2$O(cr). The consumption of Ca due to the precipitation of Ca(ox)·xH$_2$O(cr) was calculated to be <1 % of the total Ca content in the porewater of C-S-H phases with C:S = 1.4 ([Ca] = 1.8 × 10^{-2} M). This stock solution was primarily used for sorption experiments with C-S-H phases.

2.3. *Preparation and characterization of HCP, C-S-H phases and corresponding porewater solutions*

Hydrated cement paste (HCP), C-S-H phases and porewater solutions were prepared and stored in Ar-gloveboxes. Hardened cement pastes used in this work were prepared with a CEM III/C (32.5 N-LH/SR CE LA BENOR) cement provided by ONDRAF/NIRAS. Hardened cement pastes were prepared at a water-to-cement ratio (w/c) of 0.46, i.e., by mixing 315 g of dry cement with 144.4 g of Milli-Q water (quoted in the following as CEM III/C), and with 315 g of cement, 16.6 g of calcite and 152.2 g of water (quoted in the following as CEM III/C + $CaCO_3$). Both mixtures were kept in closed moulds for setting for two days and then immersed in water for curing for ca. 1.5 years. After this period, the external layer of the HCP monoliths (≈ 2.5 mm) was removed with a rotary saw to eliminate any altered outer surface. The cement block was ground by manual crushing, milled, and sieved inside an Ar-glovebox. The milling was repeatedly performed using a Pulverisette 0 equipment (Fritsch GmbH) with tungsten-carbide ball until all the material passed through a 63 μm sieve to avoid a size fractionation of the different cement phases. The inactive Nb content in HCP was quantified by total dissolution using alkaline fusion with KOH at 390 °C and ICP-MS after dilution with 2 % HNO_3.

A second batch of both HCP materials (CEM III/C and CEM III/C + $CaCO_3$) was prepared at Empa using the same w/c ratios but with a shorter curing time i.e., 91 days. The pore solution materials were used to extract the porewater by the squeezing method, and accordingly determine the porewater composition. The pore solution was extracted from paste samples hydrated for 91 days using the steel die method [38,39] and immediately filtered using 0.45 μm nylon filters. The dissolved concentrations of Na, K, Ca, Cl, SO_4, Si, and Al were quantified in three solutions diluted by a factor 10, 100, and 1000, respectively, using a Dionex DP series ICS 3000 ion chromatography (IC) system with measurement error < 10 %. The pH values were measured at ambient temperature (23 ± 2 °C) in the undiluted solution. The pH electrode was calibrated against potassium hydroxide solutions of known concentrations [40]. Based on this porewater composition and considering an overall charge balance of the solution, a preliminary recipe for the artificial cement porewater was prepared with Na_2SO_4, $Ca(OH)_2$, NaCl and corresponding volumes of 1 M NaOH and KOH. The concentration of Ca obtained in the squeezed porewater was decreased to avoid the possible precipitation of portlandite, whereas Si and Al were disregarded in the final recipe because of their low content in the squeezed porewater. The final porewater compositions considered for the HCP materials (CEM III/C and CEM III/C + $CaCO_3$) are summarized in Table 1.

A suspension of C-S-H phases with C:S = 1.4 (hereafter, C-S-H 1.4) was prepared by mixing appropriate amounts of CaO, SiO_2 (AEROSIL® 200, EVONIK), and degassed Milli-Q water. CaO was obtained by combustion of $CaCO_3$ at 1000 °C overnight, and the complete conversion confirmed by X-ray power diffraction (XRD). Due to the strong uptake expected for Nb(V), sorption experiments were prepared using a low solid-to-liquid ratio (S:L) = 0.5 g·L^{-1} (see Section 2.4). To avoid the leaching of Ca from the C-S-H phases at such low S:L, two batches with S:L = 20 g·L^{-1} were prepared and equilibrated for three weeks. The supernatant of one of the suspensions was separated by centrifugation at 3600*g* for 40 min, and afterwards used to dilute the second suspension in order to achieve the target S:L = 0.5 g·L^{-1}. The porewater composition of the C-S-H 1.4 is reported in Table 1. A second series of C-S-H samples were prepared by contacting the C-S-H paste after solid phase separation (3600 g for 40 min) with the porewater of the HCP (CEM III/C) to obtain a S:L = 0.5 g·L^{-1}.

The unhydrated CEM III/C cement was characterized by means of XRD (both at KIT and Empa) and X-ray fluorescence (XRF, only at Empa). HCP materials were also characterized by XRD (both at KIT and Empa) and differential thermogravimetric analysis (DTG, at Empa). XRD were obtained using a Bruker D8 Advance X-ray powder diffractometer with Cu anode (KIT-INE) within 2θ = 10–60°, with 0.008° incremental

Table 1
Summary of the artificial porewater compositions used in the present work for HCP materials prepared with CEM III/C and CEM III/C + $CaCO_3$, as well as the porewater composition in equilibrium with the C-S-H phases with C:S 1.4. Neither Al nor Si was added to the artificial porewater of HCP.

System	[Na] (M)	[K] (M)	[Ca] (mM)[c]	[Cl] (mM)	[SO_4^{2}] (mM)	[Al] (mM)	[Si] (mM)	pH
HCP (CEM III/C)[a]	0.071 (± 0.001)	0.078 (± 0.001)	0.92 (± 0.16)	2.4 (± 0.1)	3.5 (± 0.9)	–	–	13.1 (± 0.1)
HCP (CEM III/C + $CaCO_3$)[b]	0.070 (± 0.001)	0.122 (± 0.001)	0.71 (± 0.19)	6.5 (± 0.9)	13.7 (± 2.7)	–	–	13.1 (± 0.1)
C-S-H 1.4[d]	–	–	18.0	–	–	–	0.01	12.4

[a] Measured in the pore solution (in mM): Na: 70, K: 77 Ca: 2.9; S: 3.62, Cl: 2.1, Al: 0.1, Si: 0.09, pH 13.0.
[b] Measured in the pore solution (in mM): Na: 68, K: 71, Ca: 2.4; S: 3.2, Cl: 3.6, Al: 0.08, Si: 0.08, pH 13.0.
[c] Lowered Ca concentrations were used to avoid oversaturation with respect to portlandite.
[d] Related uncertainties are ±0.1 for pH measurements and ±10–20 % for the measured concentrations.

steps and 1 s of measurement time per step. XRD were also obtained at Empa with a Panalytical X'Pert Pro instrument with an X'Celerator detector applying CoK_α radiation ($\lambda = 1.7890$ Å) at 45 mV (voltage) and 40 mA (current). A fixed divergence slit and an anti-scatter slit on the incident beam side of ½° and 1°, respectively, were used. For quantification, Rietveld refinements were performed on the measured XRD data utilizing the Highscore Plus software 3.0.5 licensed by Panalytical. The Partial Or No Known Crystal Structure (PONKCS) method [41] was used in combination with the external standard method [42] and a determination of the bound water [43] to obtain a quantification of the degree of reaction of the cement clinker phases. The single crystal structures suggested by [44] were applied in the Rietveld refinements. The structures of cristobalite, silicon carbide and carbonated hemicarbonate were taken from [45–47], respectively. The amorphous content was quantified using calcium fluorite as external standard for derivation of the G factor [42], and the phase contents were normalized to 100 g dry binder [43].

Thermogravimetric analysis (TGA) was performed with a Mettler Toledo TGA/SDTA 8513 and a Mettler Toledo TGA2 (sample after 730 d of hydration, and the CEM III/C and CEM III/C + LS after 91d only) instruments. Approximately 50 mg sample was investigated in the temperature range 30–980 °C with a heating rate of 20 K/min and in a N_2 atmosphere.

2.4. Sorption experiments with ^{95}Nb and ^{93}Nb isotopes

Sorption experiments were conducted with ^{95}Nb (active), ^{93}Nb (inactive) and a combination of both. Besides the active stock solutions described in Sections 2.2.1 and 2.2.2, a stock solution containing [^{93}Nb (V)] = 2.25×10^{-2} M was prepared dissolving $NbCl_5$ in a NaOH / KOH solution of the same composition and pH as the porewater of the HCP (CEM III/C, see Table 1) but excluding Ca.

Sorption samples were prepared and stored in HDPE vials (Zinsser Analytic) and PP narrow neck bottle (Kautex) for HCP and C-S-H systems, respectively. The binary sorption systems ("HCP-Nb" and "C-S-H-Nb") were investigated at S:L = 0.5 g·L^{-1}, $C_0 = 5 \times 10^{-9}$ M – 1×10^{-5} M, and A(^{95}Nb)$_0$ = 31 kBq (HCP samples) or A(^{95}Nb)$_0$ = 3.6 kBq (C-S-H 1.4 samples). A series of samples containing only inactive niobium, i.e., [^{93}Nb] = 2×10^{-7} M – 1×10^{-3} M, was prepared under the same conditions as the active samples. The leaching of ^{93}Nb from HCP was determined after contacting HCP with the artificial porewater at S:L = 0.5 g·L^{-1} for two weeks. The impact of ISA on the uptake of Nb by HCP (system "HCP-Nb/ISA") was investigated by batch sorption experiments performed with S:L = 0.5–2 g·L^{-1}, $C_0 = 5 \times 10^{-9}$ M, A(^{95}Nb)$_0$ = 10 kBq and 10^{-5} M ≤ [ISA]$_0$ ≤ 0.1 M. Sorption samples "HCP-Nb/ISA" were prepared following two different sequences for the addition of the individual components, i.e., "(HCP + Nb) + ISA" and "(Nb + ISA) + HCP", where the two components in parenthesis were pre-equilibrated for 2 days before the addition of the third component.

The effect of chloride on the uptake of Nb(V) (system "HCP-Nb/Cl") was investigated by a series of batch sorption experiments at S:L = 0.5 g·L^{-1}, $C_0 = 5 \times 10^{-9}$ M, A(^{95}Nb)$_0$ = 31 kBq and 2.4×10^{-3} M ≤ [Cl]$_0$ ≤ 2 M. The lowest chloride concentration was defined by the chloride content in the porewater of HCP (CEM III/C and CEM III/C + $CaCO_3$). A NaCl stock solution was prepared by dissolving the given amount of NaCl in the corresponding porewater solutions. The uptake of Cl by HCP was quantified as negligible at S:L = 0.5 g·L^{-1}. The uptake of Nb(V) in the quaternary system "HCP-Nb/ISA/Cl" was investigated with a series of sorption experiments with 2.4×10^{-3} M ≤ [Cl]$_0$ ≤ 2 M, [ISA]$_0$ = 3.2×10^{-2} M, S:L = 0.5 g·L^{-1}, $C_0 = 5 \times 10^{-9}$ M, and A(^{95}Nb)$_0$ = 10 kBq. ISA was added to the suspension after 2 days of pre-equilibration of HCP with Nb and Cl , i.e., following the order of addition "(HCP + Nb + Cl) + ISA". Table 2 summarizes the experimental conditions in the sorption systems investigated in this work.

All samples were continuously agitated using an orbital shaker (VXR basic Vibrax, IKA). After the corresponding contact time, about 4 mL of the supernatant was transferred to PP ultracentrifugation tube (Beckman Coulter), heat-sealed inside the glovebox and transferred to an ultracentrifuge for phase separation (ca. 600,000 g for 1 h, Optima XPN-90, Beckman Coulter). After ultracentrifugation, 2.8–3.2 mL of the

Table 2
Experimental conditions in the Nb(V) sorption experiments conducted in this work.

System	Cement type / phase	C_0 ([Nb]$_0$ / M)	S:L (g·L^{-1})	[Cl(M)][a]	[ISA(M)]	Activity of ^{95}Nb (kBq and M)
HCP-Nb	CEM III/C CEM III/C + $CaCO_3$	5×10^{-9} M – 1×10^{-5} M	0.5	2.4×10^{-3} M and 6.5×10^{-3} M	–	31 kBq (2.2×10^{-10} M)
HCP-Nb/ISA	CEM III/C CEM III/C + $CaCO_3$	5×10^{-9} M	0.5–2	2.4×10^{-3} M and 6.5×10^{-3} M	10^{-5} M – 10^{-1} M	10 kBq (7.2×10^{-11} M)
HCP-Nb/Cl	CEM III/C CEM III/C + $CaCO_3$	5×10^{-9} M	0.5	$[Cl]_{PW}$ – 2 M	–	31 kBq (2.2×10^{-10} M)
HCP-Nb/ISA/Cl	CEM III/C CEM III/C + $CaCO_3$	5×10^{-9} M	0.5	$[Cl]_{PW}$ – 2 M	3.2×10^{-2} M	10 kBq (7.2×10^{-11} M)
C-S-H-Nb	C-S-H 1.4	9.1×10^{-11} M – 5.6×10^{-3} M	0.5	–	–	3.6 kBq (2.6×10^{-11} M)

[a] $[Cl]_{PW}$ 2.4×10^{-3} M and 6.5×10^{-3} M correspond to the concentration of chloride in the porewater in equilibrium with hardened cement pastes of CEM III/C and CEM III/C + $CaCO_3$, respectively.

supernatant (precise volume depending upon sample) were recovered and diluted in 2 % HNO_3 for gamma spectrometry. The detection limit of the gamma measurements for ^{95}Nb was 0.04–0.16 Bq/mL for a measuring time of 4 h, which corresponds to [^{95}Nb] = 9.7 × 10 ^{13} M – 3.9 × 10 ^{12} M considering the corresponding dilution factors. The sorption of ^{95}Nb on the walls of HDPE and PP vessels was evaluated at different activities of ^{95}Nb and total concentrations of niobium. All sorption values reported in this work are corrected for this effect. Distribution ratios calculated for experiments using only ^{93}Nb, $R_{d,^{93}Nb}$ (in L·kg ^{1}), were calculated as follows:

$$R_{d,^{93}Nb} = \frac{C_{solid}}{C_{aq}} = \frac{C_0 \quad C_{aq}}{C_{aq}} \cdot \frac{V}{m} \tag{1}$$

where C_{solid} is the concentration of ^{93}Nb in the solid phase (in mol·kg ^{1}), C_{aq} is the concentration of ^{93}Nb in the aqueous phase (in mol·L ^{1}), C_0 is the initial concentration of ^{93}Nb (in mol·L ^{1}), V is the sample volume (in L) and m is the mass of HCP or C-S-H (in kg). On the other hand, the distribution ratios determined from the experiments containing ^{95}Nb, $R_{d,^{95}Nb}$, were determined as follows:

$$log\ R_{d,^{95}Nb} = \frac{A_0(^{95}Nb) \quad A_{aq}(^{95}Nb)}{A_{aq}(^{95}Nb)} \cdot \frac{V}{m} \tag{2}$$

where A_0(^{95}Nb) is the initial activity of ^{95}Nb and A_{aq}(^{95}Nb) is the activity of ^{95}Nb in the aqueous phase after sorption.

Uncertainties in C_{solid}, C_{aq}, A_{aq}(^{95}Nb), and R_d values were calculated as the standard deviation of average values obtained from replicated samples. For those sample for which only single measurements were available, average uncertainties of ±0.5 and ± 0.4 were applied for log R_d (with R_d in L·kg ^{1}) of CEM III/C and CEM III/C + $CaCO_3$, respectively, which were the maximum uncertainties obtained from replicated samples in each system.

Nb solubility in the porewater of HCP was determined from oversaturation conditions using inactive ^{93}Nb with C_0 = 1 × 10 ^{5} M – 5 × 10 ^{4} M. After 35 and 119 days, the aqueous phase was separated with 10 kDa ultrafiltration (Nanosep® centrifugation tube, Pall Life Science) and diluted in 2 % HNO_3 for the quantification of ^{93}Nb by ICP-MS.

3. Results and discussion

3.1. Characterization of hydrated cement and C-S-H phases

The composition of the unhydrated cement was also characterized by XRF and XRD (Table SI-1 in the Supporting Information). A slag content of 84 wt% was determined in the unhydrated cement (see section 1.4 in Supporting Information). Alite (3CaO·SiO_2 (C_3S), hatrurite, PDF 86-0402), anhydrite ($CaSO_4$, PDF 72-0503) and belite (2CaO·SiO_2 (C_2S), larnite, PDF 09-0351) were the most abundant crystalline phases identified in the unhydrated cement. Rietveld analysis of the XRD and the comparison with XRF data revealed also the presence of small fractions of aluminate, ferrite, hemihydrate, gypsum, calcite, quartz and gehlenite (all below 0.5 % w/w), as well as a large fraction of amorphous material (88.4 %). Diffractograms collected for the hydrated HCP materials (Fig. 1) showed patterns corresponding to ettringite ($Ca_6Al_2(SO_4)_3(OH)_{12}\cdot 26H_2O$, PDF 41-1451) and hydrotalcite ($Mg_6Al_2CO_3(OH)_{16}\cdot 4H_2O$, PDF 14-0191) as well as the broad signal at 2θ ≈ 30° indicating the presence of C-S-H. Calcite ($CaCO_3$, PDF 5-586) was present only in traces in CEM III/C but clearly in CEM III/C + $CaCO_3$, else no significant difference was observed between the two cements. The TGA results indicate the presence of mainly C-S-H and ettringite as well some hydrotalcite and possibly some AFm phases such as hemicarbonate and again only traces of carbonates in CEM III/C (Fig. SI-4 in the Supporting Information). Portlandite was absent, due to the low Portland cement content of 16 wt% and the partial reaction of the slag as a

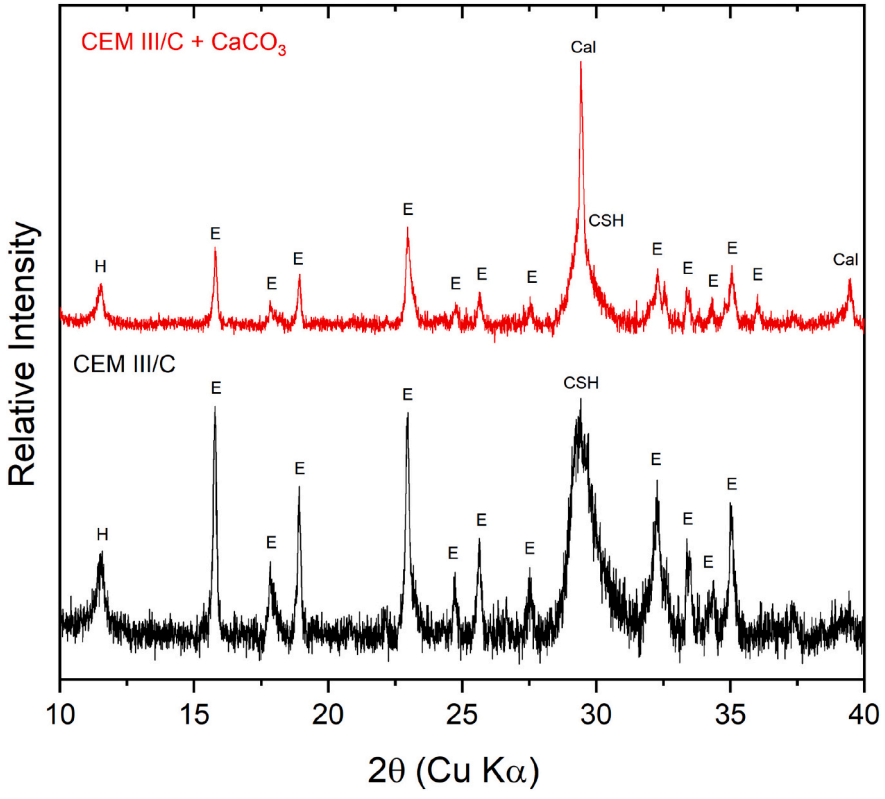

Fig. 1. X-ray diffraction (XRD) patterns of hardened cement paste powders of CEM III/C and CEM III/C + $CaCO_3$. Peaks in diffractograms are assigned and labelled with selected references available in the Joint Committee on Powder Diffraction Standards database [48]. Nomenclature in the figure: Cal: calcite; E: ettringite; H: hydrotalcite.

reaction degree of 50 % of the slag is expected after 1.5 years of hydration (see section 1.4 in Supporting Information). Due to the presence of blast furnace slag the CEM III/C and CEM III/C + $CaCO_3$ studied here contain a high content of C-S-H and hydrotalcite, but no portlandite and no significant amount of AFm phases in contrast to the Portland cement (CEM I) studied in [33].

The Nb content in pristine HCP was quantified as (7.1 ± 0.7) and (7.6 ± 0.9) ppm (corresponding to (7.6 ± 0.8) × 10^{-5} and (8.1 ± 0.9) × 10^{-5} mol·kg^{-1}) for CEM III/C and CEM III/C + $CaCO_3$, respectively. These concentration values are slightly higher but of the same order as the Nb content previously determined for CEM I, i.e., (3.1 ± 0.3) ppm [33]. The reference book by Ochs and co-workers cited a comparable Nb content of 7.6, 5.1 and 5.3 ppm in CEM I, CEM III/B and CEM III/C, respectively [10].

3.2. Nb(V) retention in HCP and C-S-H 1.4 systems

The solubility of Nb(V) in the porewater solutions of HCP (CEM III/C and CEM III/C + $CaCO_3$) was determined from oversaturation conditions with 1 × 10^{-5} M ≤ C_0 ≤ 5 × 10^{-4} M. The quantification of Nb concentration in the aqueous phase (C_{aq}) after equilibration times of ≤120 days ranged between <2.7 × 10^{-9} M (detection limit of ICP-MS in the conditions of this study) and 2.8 × 10^{-8} M. Measured Nb concentrations after attaining equilibrium were independent of C_0, and showed no clear differences for experiments conducted with porewater solutions of CEM III/C and CEM III/C + $CaCO_3$. Although the amount of solid phase obtained in these experiments was insufficient for appropriate solid phase characterization, the significant drop in the niobium concentration can be explained by the precipitation of Ca-Nb(V) (oxo-)hydroxides, expectedly pyrochlores of the type $Ca_2Nb_2O_7$(cr), as recently proposed for cementitious systems [32].

Kinetics for the uptake of Nb(V) by HCP (CEM III/C and CEM III/C + $CaCO_3$) and C-S-H 1.4 were monitored for t ≤ 15 days, and confirmed that steady state is achieved within only 2 days for all the investigated systems (see Fig. SI-5 in the Supporting Information). This is in line with our previous study with HCP (CEM I) [33].

Following the results from the kinetic experiments, sorption isotherms for the uptake of Nb(V) by HCP (CEM III/C and CEM III/C + $CaCO_3$) and C-S-H 1.4 were determined after 5 days of contact time (Fig. 2). Additional measurements at t = 43 days were conducted for selected CEM III/C and C-S-H 1.4 samples with Nb(V) concentrations above the solubility limit of (expectedly) Ca-Nb(V) oxide phases (see dashed lines in Fig. 2). Upper solubility limits of Nb(V) in the corresponding porewaters were experimentally determined in this work for CEM III/C (< 2.8 × 10^{-8} M) and in Jo et al. [32] for a porewater analogous to C-S-H 1.4 (< 10^{-8} M). Total concentrations of Nb(V) in the aqueous phase (C_{aq}) were determined by ICP-MS (direct quantification) in the sorption experiment using only stable ^{93}Nb, whereas Eq. (3) was used to calculate C_{aq} in the sorption experiments containing ^{93}Nb and ^{95}Nb:

$$C_{aq} = \frac{A_{aq}(^{95}Nb)}{A_0(^{95}Nb)} \cdot C_0 \quad (3)$$

where C_0 is the initial aqueous concentration of Nb(V) including active and inactive isotopes, A_{aq}(^{95}Nb) is the activity of ^{95}Nb remaining in aqueous phase after sorption, and A_0(^{95}Nb) is the initial activity of ^{95}Nb. In HCP samples, the inventory of ^{93}Nb in pristine cement was considered for the calculation of C_{solid} (Nb concentration in solid phase). For selected samples containing ^{93}Nb and ^{95}Nb, C_{aq} at t = 5 days was determined by means of both ICP-MS and gamma spectrometry. The comparison confirmed the excellent agreement between the C_{aq} determined with both methods (e.g., 1.8 × 10^{-7} M and 2.4 × 10^{-7} M by ICP-MS and gamma spectrometry, respectively).

Concentration of ^{93}Nb in the porewater equilibrated with pristine HCP (CEM III/C) systems with S:L = 0.5–2 g·L^{-1} was below the detection limit of ICP-MS (2.7 × 10^{-9} M within the considered experimental conditions). For this reason, the contribution of leached ^{93}Nb was disregarded for the calculation of C_{aq}.

Sorption isotherms determined for HCP and C-S-H 1.4 at t = 5 days show a linear trend with slope ≈ 1. A slight deviation from this linearity is observed for HCP systems with C_{aq} < 10^{-10} M. This is likely because the contribution of ^{93}Nb leached from HCP (< detection limit of ICP-MS) to the total concentration of niobium in the aqueous phases (C_{aq}) was not considered. In line with this hypothesis, note that previous studies conducted with HCP (CEM I) in the degradation stage I have reported concentrations of ^{93}Nb in the cement porewater ranging from 8 × 10^{-10} M [33] to 1.3 × 10^{-9} M [31]. Moreover, we note that at such low Nb(V) inventories, the calculated concentration of niobium in the solid phase is mostly dominated by the inventory of ^{93}Nb in pristine cement (see dashed horizontal line in Fig. 2).

Experiments with C-S-H phases overcome the intrinsic difficulties in HCP caused by the presence of ^{93}Nb in pristine cement. Hence, sorption isotherms determined for C-S-H 1.4 follow a linear trend over almost nine orders of magnitude (at t = 5 days) in terms of niobium aqueous concentration, i.e., 10^{-14} M ≤ C_{aq} ≤ 10^{-5} M. This observation clearly endorses the concept of constant distribution coefficient, R_d, to explain Nb(V) uptake, i.e., $logC_{solid} = logC_{aq} + logR_d$.

No apparent differences in the sorption properties of the HCP materials investigated (CEM III/C and CEM III/C + $CaCO_3$) were observed in experiments using ^{95}Nb, and thus an average value of $log\ R_{d,^{95}Nb}$ = (5.5 ± 0.6) (with R_d in L·kg^{-1}) is calculated for these systems. Almost identical R_d values are calculated from experiments using only ^{93}Nb, i.e., $log\ R_{d,^{93}Nb}$ = (5.6 ± 0.3). The accurate determination of both $log\ R_{d,^{95}Nb}$ and $log\ R_{d,^{93}Nb}$ allows to gain insight on the relevance of isotopic exchange with ^{93}Nb in pristine cement as mechanism for the uptake of radioactive isotopes of niobium (^{95}Nb in this study, ^{94}Nb under repository conditions). For this purpose, the partition coefficient (α) is calculated according to Eq. (4):

$$\alpha = \frac{\left(n_{solid,^{95}Nb}/n_{solid,^{93}Nb}\right)}{\left(n_{aq,^{95}Nb}/n_{aq,^{93}Nb}\right)} = \frac{R_{d,^{95}Nb}}{R_{d,^{93}Nb}} \quad (4)$$

where n represents the amount (in mole) of ^{95}Nb and ^{93}Nb in solid and aqueous phases [49]. The α refers to the ratio of isotopic concentration between two phases, and reflects the availability of ^{93}Nb in the solid phase for isotopic exchange with ^{95}Nb originally only present in the aqueous phase. A value of α ≈ 1 indicates a full availability of ^{93}Nb for isotopic exchange, whereas α < 1 supports that such an exchange was not fully achieved in the course of the experiments.

Considering the values of $R_{d,^{95}Nb}$ and $R_{d,^{93}Nb}$ determined in this work, a value of α ≈ 1 is calculated. This supports (i) that ^{93}Nb in pristine cement is fully available for isotopic exchange, at least under the conditions investigated in the present study, and thus (ii) that isotopic exchange with ^{93}Nb is possibly a relevant mechanism for the uptake of other isotopes of niobium (e.g., ^{95}Nb in this experiment or ^{94}Nb in repository).

Additional insight on the mechanism/s driving the uptake of niobium in cementitious systems can be extracted from the comparison of sorption data in HCP and C-S-H systems. Hence, similar but slightly higher R_d values are determined for the uptake of niobium by C-S-H phases, as compared to HCP materials (i.e., $log\ R_{d,^{95}Nb}$ = (5.5 ± 0.6) and (6.5 ± 0.3) for HCP and C-S-H phases, respectively). This observation supports that the uptake by C-S-H phases is a prevalent mechanism in the retention of niobium in cement systems. C-S-H phases represent approximately 50 % of the total weight in HCP, which can explain the greater R_d values in C-S-H if C-S-H phases act as main sink of Nb. Differences in the surface area of both materials (i.e., ≈ 150 m^2·g^{-1} for C-S-H phases [50], ≈ 50–80 m^2·g^{-1} for HCP [34,51]) are expected to contribute as well to such differences. The $log\ R_{d,^{95}Nb}$ = (6.5 ± 0.3)

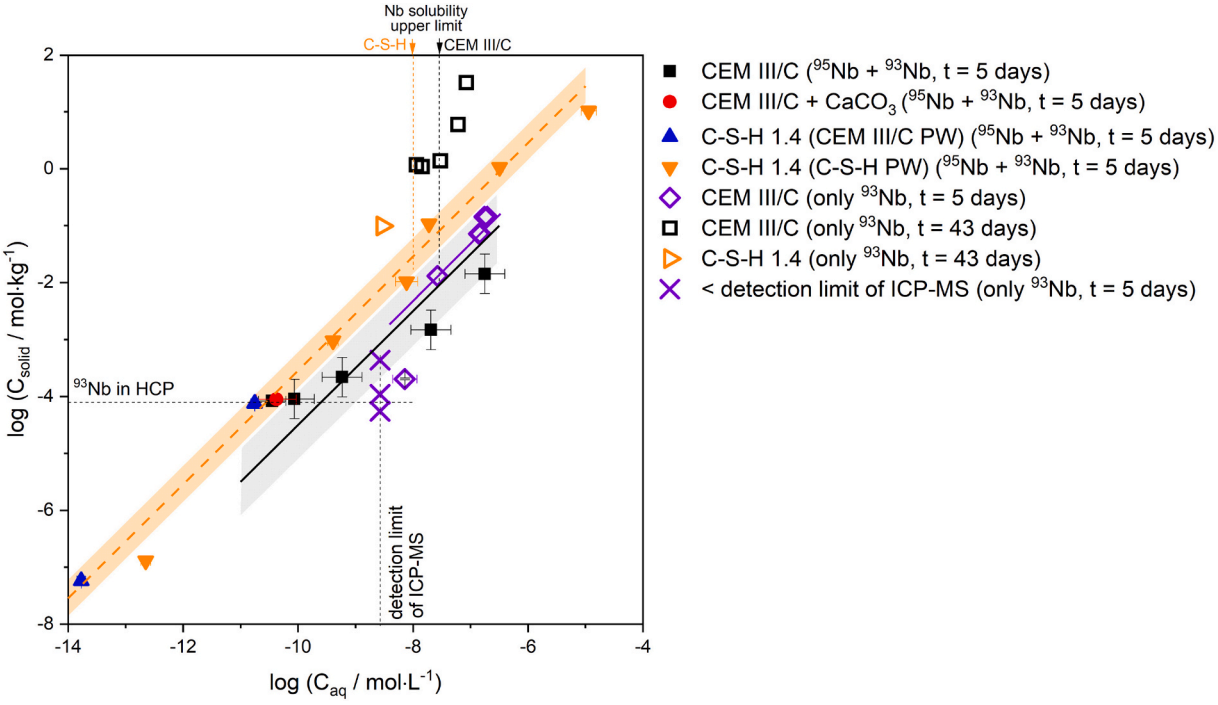

Fig. 2. Nb(V) sorption isotherms for the uptake of Nb(V) by HCP (CEM III/C and CEM III/C + $CaCO_3$) and C-S-H 1.4 (equilibrated with C-S-H 1.4 and CEM III/C porewater solutions) at t 5 and 43 days. Distribution coefficients reported in the figure were obtained with the measurements at t 5 days: log R_d (5.5 ± 0.6), (5.6 ± 0.6), and (6.5 ± 0.3) for experiments using ^{93}Nb + ^{95}Nb with HCP, only ^{93}Nb with HCP, and ^{93}Nb + ^{95}Nb with C-S-H 1.4, respectively. The lines of $logC_{solid}$ $logC_{aq}$ + R_d, and uncertainty area corresponding to the given R_d are indicated. Solubility upper limits of Nb in CEM III/C and C-S-H 1.4 (expectedly defined by Ca-Nb (V) oxide phases) are given as dashed lines, as determined experimentally in this work or reported in Jo et al. (2022) [32]. Detection limit of ICP-MS for ^{93}Nb in the conditions of this study is provided as reference. Horizontal dashed line indicates the concentration of ^{93}Nb in pristine cement. Detail of the experimental conditions are summarized in Table 1. All experimental data points are summarized in Table SI-2 of the Supporting Information.

determined in this work for C-S-H phases is comparable with R_d values reported for other metal ions characterized by strong hydrolysis, i.e., Be (II), An(III), An(IV), Sn(IV), Np(V) or U(VI) among others, with $log\ R_d \approx$ 5–6 [23,24,52–54]. Surface sorption and incorporation in the interlayer of C-S-H have been identified as the main mechanism for the uptake of radionuclides uptake by C-S-H [23,25,55].

At longer contact times (t = 43 days), the concentration of niobium in the solid phases in those samples with C_{aq} > Nb(V) solubility limit (dashed lines in Fig. 2, as determined experimentally in this work for CEM III/C and in Jo et al. [32] for C-S-H 1.4) increases, thus deviating from the linear trend in the sorption isotherm. This behaviour is representative of solubility phenomena, which in the longer term is

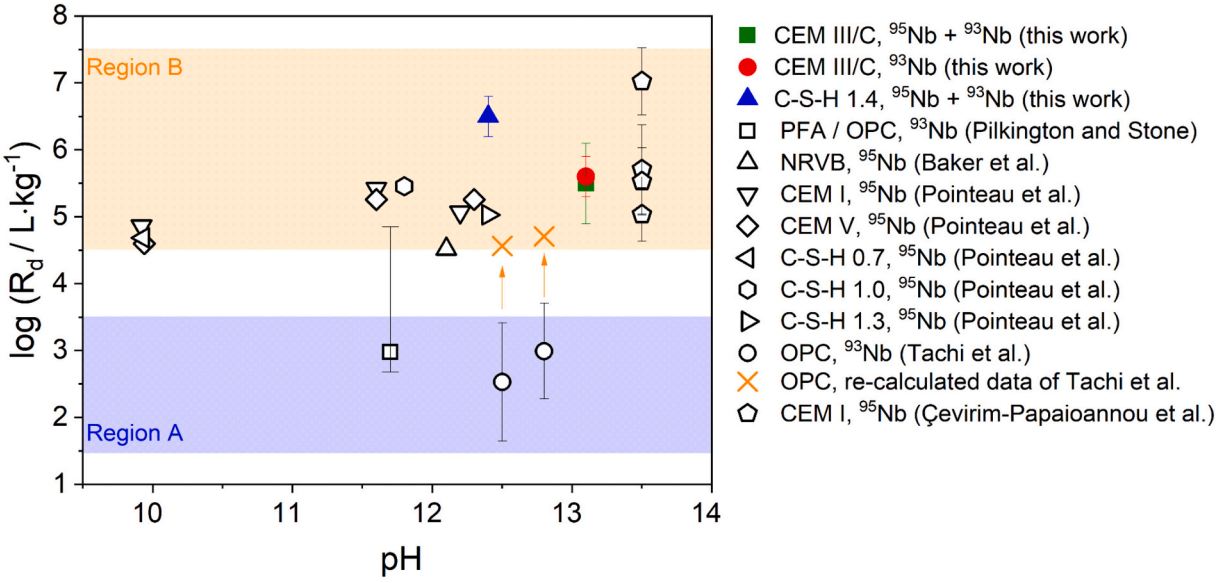

Fig. 3. Distribution coefficients (R_d) of Nb(V) on HCP and C-S-H phases as determined in this work or reported by Pilkington and Stone (1990) [28], Baker et al. (1994) [29], Pointeau et al. (2004) [30], Tachi et al. (2020) (original data [31] and re-calculated in this work assuming 5 ppm ^{93}Nb content in OPC), and Çevirim-Papaioannou et al. (2022) [33]. See description for Regions A and B in the text.

expectedly controlling C_{aq} for those systems above the solubility limit.

Distribution coefficients of Nb(V) determined in this work for HCP and C-S-H phases are summarized in Fig. 3 as a function of pH, together with data previously reported in the literature. Independently of the pH, distribution coefficients in the figure are grouped in two main regions, at log $R_d \approx (3 \pm 1)$ [28,31] and log $R_d \approx (6 \pm 1)$ (this work and [29,30,33]). All experiments in region A were conducted with ^{93}Nb, whereas sorption studies in region B used ^{95}Nb with the exception of one experimental series conducted in this work with only ^{93}Nb. Tachi and co-workers conducted their sorption experiments at low initial niobium concentrations of ^{93}Nb ($C_0 = 2.1 \times 10^{-8}$ M), and calculated the distribution coefficients considered the partitioning of this initial concentration between the solid and aqueous phases, resulting in log R_d values of 2–3 [28,31]. The authors did not consider the content of ^{93}Nb in pristine cement, which at such low Nb inventories can have a significant impact in the calculation of the R_d. Hence, a recalculation of the distribution coefficient from data in Tachi et al. but considering a range of ^{93}Nb content of 1–10 ppm in cement results in log $R_d \approx$ 4–5, thus more in line with sorption data in region B. The second study in region A was conducted by Pilkington and Stone, who investigated the uptake of ^{93}Nb by a 10:1 mixture of Pulverised Fuel Ash / Ordinary Portland Cement (PFA / OPC) [28]. The porewater in equilibrium with this cement material was characterized by pH = 11.8 and a relatively low calcium concentration, i.e., [Ca] $= 9.2 \times 10^{-4}$ M. In contrast to Tachi and co-workers, sorption experiments by Pilkington and Stone were conducted with very high initial niobium concentrations, i.e., $C_0 = 5.3 \times 10^{-3}$ M. After contact times of 1–2 months, the authors reported very disperse distribution coefficients ($R_d = 5 \times 10^2$–8×10^4 L·kg^{-1}). We hypothesize that, at the high C_0 considered in [28], solubility phenomena is responsible for the observed decrease in the concentration of niobium. In our recent solubility study, we reported Nb(V) concentrations of $\approx 10^{-8}$ M at pH = 11.5 and [Ca] $= 1 \times 10^{-3}$ M, i.e., under boundary conditions very similar as those considered by Pilkington and Stone. Moreover, these authors reported a systematic decrease of R_d values with increasing S:L ratios,[2] which again may hint towards solubility phenomena: the concentration of niobium in the aqueous phase remains nearly constant, and the systematic decrease in the R_d values is given by the division by S:L.

Sorption experiments conducted with the short-lived isotope ^{95}Nb were performed at low niobium concentrations (this work and [29,30,33]), thus allowing the quantification of very low metal concentrations and avoiding the problematic associated with Nb(V) solubility phenomena. Sorption experiments conducted in this work with ^{93}Nb were performed within a narrow experimental window, defined by the detection limit of ICP-MS (lower limit) and the solubility limit of the Ca-Nb(V)-OH(s) solid phases precipitating under the investigated conditions (upper limit). This allows the correct determination of the $R_{d,^{93}Nb}$, in line with all experiments using ^{95}Nb in region B of Fig. 3. On the basis of these observations, we conclude that previous studies reporting log $R_d \approx 3$ largely underestimate the uptake of niobium by cementitious systems, which shows instead a very strong sorption with log $R_d \approx (6 \pm 1)$. The cement composition itself, seems to have little impact on the Nb sorption.

3.3. Impact of ISA on the uptake of Nb(V) by HCP

Fig. 4 shows the impact of ISA on the uptake of Nb(V) by CEM III/C and CEM III/C + $CaCO_3$, expressed in terms of log R_d values as a function of log $[ISA]_{tot}$. Full symbols correspond to the order of addition of the individual components "(HCP + Nb) + ISA", whereas the empty symbol at log $[ISA]_{tot} =$ 2 represents the order of addition "(Nb + ISA) + HCP" (see further details in Section 2.4). For both HCP materials, sorption data clearly show a significant decrease of R_d values at $[ISA]_{tot} > 10^{-3}$ M. The greatest impact is observed at $[ISA]_{tot} = 0.1$ M, for which R_d values decrease ca. 2 orders of magnitude with respect to the ligand-free system. These results are consistent with data obtained in our previous study with HCP (CEM I) at pH = 13.5 [33].

The decreased sorption of Nb(V) with increasing ISA concentrations is explained by the formation of stable (Ca-)Nb(V)-ISA complexes in the aqueous phase. Similar observations have been reported for the uptake of other radionuclides by HCP in the presence of ISA, e.g., Th(IV), Pu(III/IV) or Am(III) [22,34]. No experimental studies are available in the literature investigating the complexation of Nb(V) with ISA in alkaline conditions, but the formation of strong complexes with ISA has been extensively reported for actinides (e.g., Th, U, Np, Pu, Am), fission (e.g., Tc, Zr) and activation products (e.g., Ni) [15,18–21,56–58]. The interpretation of the sorption experiments for the ternary system HCP-Nb(V)-ISA requires as well an appropriate understanding of the binary system HCP-ISA. Several studies have confirmed a moderate uptake of ISA by HCP, which can alter the surface properties of HCP and decrease the free ligand concentration in solution available for complexation [34,59–61]. Molecular dynamics calculations suggest that the bridging calcium in C-S-H phases is responsible for the uptake of both ISA [61] and metal ions (e.g., Be(II) [62], U(VI) [63]). Sorption experiments conducted with HCP (CEM III/C and CEM III/C + $CaCO_3$) and ISA at 0.5 g·L^{-1} ≤ S:L ≤ 2 g·L^{-1} revealed a minor decrease of the initial ISA concentration, and accordingly that $[ISA]_{tot} \approx [ISA]_{free}$. This observation refers to the conditions of our study, but does not apply to higher S:L ratios, where a significant drop in the concentration of ISA is expected (see data in [61] for HCP (CEM I) / ISA system).

Dashed lines in Fig. 4 represent the fraction of CaO (%, right y-axis) remaining in HCP as a function of log $[ISA]_{tot}$, calculated for the different S:L ratios investigated in this work. These curves give insight on the stability of HCP with increasing ligand concentrations. Calculations are performed using the NEA-TDB thermodynamic selection [64], and account for the formation of Ca-OH-ISA complexes and the corresponding dissolution of CaO from HCP. Solubility calculations indicate that for experiments conducted at S:L = 0.5 g·L^{-1}, ca. 70 % of the CaO in HCP is expectedly dissolved at $[ISA]_{total} = 0.1$ M. The solubility limit of $Ca(ISA)_2$ reached only at $[ISA]_{total} = 0.1$ M was considered in the estimation of the amount of CaO dissolution. These calculations are qualitatively confirmed by the Ca concentration experimentally determined in the aqueous phase (see Table SI-3[3] in Supporting Information). Although thermodynamic equilibrium is expectedly not attained within the timeframe of the sorption experiments, the calculated % CaO are considered as criteria to disregard the results obtained for the most extreme case, i.e., S:L = 0.5 g·L^{-1} and $[ISA]_{total} = 0.1$ M (symbol in brackets in Fig. 4).

The effect of the order of addition of the individual components was assessed at $[ISA]_{tot} = 10^{-2}$ M, S:L = 0.5 g·L^{-1} and t = 5 days. Hence, the sequence "(Nb + ISA) + HCP" resulted in clearly lower R_d values (ca. 1.5 orders of magnitude) compared to the reference sequence "(HCP + Nb) + ISA". These observations agree with previous investigations on the systems HCP-Pu/ISA [34] and HCP-Nb/ISA (with CEM I) [33]. Although the trends reported by Tasi et al. on the HCP-Pu-ISA system are in line with ours at short contact times, long-term experiments conducted by the authors with the long-lived isotope ^{242}Pu confirmed that the sequence "(Pu + ISA) + HCP" is kinetically hindered [34]. Hence, R_d values determined for this sequence systematically increased with time, until eventually meeting R_d values determined for the sequence "(HCP + Pu) + ISA" after long equilibration times (t = 490 days). A similar

[2] The authors reported R_d values (only upper limits listed) of 8.1×10^4, 7.6×10^4, 6.5×10^4, 8.2×10^3, 1.0×10^4 and 3.3×10^3 L·kg^{-1} at S:L 5, 10, 15, 20, 30 and 40 g·L^{-1}, respectively.

[3] Measurements of the Ca concentration correspond to experiments conducted in the absence of Nb. Measurements were conducted at t 20 days, and thus do not necessarily capture the state of HCP within the timeframe of the sorption experiments, i.e., t 5 days.

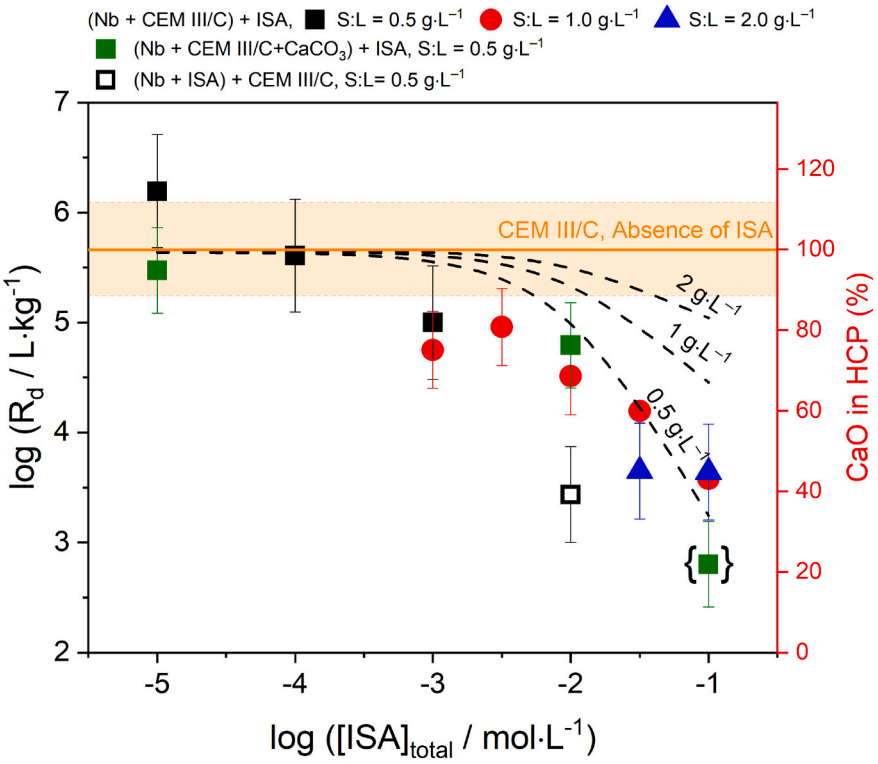

Fig. 4. Impact of isosaccharinic acid (ISA) on the uptake of Nb(V) (expressed as R_d values) by HCP (CEM III/C and CEM III/C + $CaCO_3$). Solid line and orange region show the R_d of Nb(V) in HCP (CEM III/C) and corresponding uncertainty in the absence of ISA. The terms "(Nb + HCP) + ISA" and "(Nb + ISA) + HCP" indicate the order of addition of the individual components. The two components in parenthesis were pre-equilibrated for 2 days before the addition of the third component. Dashed curves represent the fraction of CaO (%) in HCP as a function of log $[ISA]_{tot}$, calculated at S:L 0.5, 1, and 2 g·L^{-1}. All experimental data corresponding to t 5 days after the addition of the third component. Further experimental details are summarized in Table 1 ("HCP-Nb/ISA"). All data points and corresponding uncertainties are provided in Table SI-4 in Supporting Information.

behaviour is expected for Nb.

3.4. Impact of chloride on the uptake of Nb(V) in the ternary HCP-Nb/Cl and quaternary HCP-Nb/ISA/Cl systems

Fig. 5 shows the evolution of the R_d values for the uptake of Nb(V) by HCP as a function of NaCl concentration in the absence (figure a) and presence (figure b) of ISA. The chloride concentration considered in the experiments spanned from the intrinsic [Cl] in the cement porewater (2.4×10^{3} M and 6.5×10^{3} M for CEM III/C and CEM III/C + $CaCO_3$, respectively) to 2 M. Fig. 5 confirms that [NaCl] < 2 M has a negligible effect on the uptake of Nb(V) by HCP, both in the absence and presence of ISA. These results are in line with our previous observations for CEM I [33]. Previous studies have shown a significant sorption of Na by C-S-H phases with low C:S ratios, resulting in a relevant increase of Ca concentration in the porewater [65–67]. However, a much weaker sorption was reported in the high C:S ratios investigated in this work. Moderate to high concentrations of chloride in the porewater have been shown to promote the transformation of AFm phases into Friedel's salt [10,61,68]. However, AFm phases are expected to play a minor role in the uptake of Nb, and thus their transformation to Friedel's salt should have no significant impact in the investigated system. These results confirm that chloride has a negligible effect on the retention of Nb(V) by HCP in the degradation stage I, even in the high concentrations expected in the evaporator concentrates disposed in specific waste streams in L/ILW.

4. Summary and conclusions

The uptake of Nb by HCP (CEM III/C and CEM III/C + $CaCO_3$) and C-S-H phases with a Ca:Si ratio of 1.4 was studied with a comprehensive series of sorption experiments using a combination of ^{93}Nb (inactive) and the short-lived isotope ^{95}Nb ($t_{1/2}$ = 35.0 days). Experiments were performed under Ar atmosphere with HCP in the degradation stage I (representing young and fresh cement hydrates) at pH = 13.1. The use of ^{95}Nb allows the detection of trace Nb concentrations by gamma spectrometry (detection limit ≈ 1×10^{12} M ^{95}Nb), which is required due to the strong sorption and the possible precipitation of sparingly soluble Ca-Nb(V) oxides at $C_0 > 10^{8}$ M. The impact of isosaccharinic acid and chloride (both relevant components in specific waste streams in L/ILW repositories) on the uptake of Nb was also investigated at 10^{5} M ≤ $[ISA]_{tot}$ ≤ 0.1 M and 2.4×10^{3} M ≤ [NaCl] ≤ 2.0 M.

The content of ^{93}Nb in pristine HCP was determined as (7.1 ± 0.7) ppm and (7.6 ± 0.9) ppm for CEM III/C and CEM III/C + $CaCO_3$, respectively. The concentration of ^{93}Nb in the porewater equilibrated with HCP systems with S:L = 0.5–2 g·L^{1} was below the detection limit of ICP-MS (2.7×10^{9} M within the considered experimental conditions).

Sorption kinetic experiments show that steady-state is attained after 2 days of contact time. A strong uptake is observed for HCP and C-S-H phases, with log R_d = (5.5 ± 0.6) and (6.5 ± 0.3), respectively (R_d values in L·kg^{1}). These observations support that C-S-H phases are the main sink of niobium in cement systems. Linear sorption isotherms are obtained over almost eight orders of magnitude in terms of niobium concentration (10^{14} M ≤ C_{aq} ≤ 10^{5} M) for C-S-H phases, but this range is limited in HCP systems due to the presence of ^{93}Nb in pristine cement. Indeed, isotopic exchange of ^{95}Nb (this study) or ^{94}Nb (repository conditions) with ^{93}Nb in cement should be additionally considered as a feasible retention mechanism of niobium in repositories for L/ILW. For the first time, and accurate quantification of $log\, R_{d,^{93}Nb}$ in HCP was achieved within the narrow experimental window defined by the detection limit of ICP-MS, the solubility limit of niobium in the cement porewater, as well as considering the content of ^{93}Nb in pristine cement and corresponding porewater. This value is in excellent agreement with the distribution coefficient determined in sorption experiments with ^{95}Nb, thus allowing to shed light on the discrepancies existing in the literature between experiments conducted with ^{95}Nb and ^{93}Nb.

The presence of ISA in cement porewater decreases significantly the uptake of Nb(V) by HCP, although a significant sorption (log R_d ≈ 3.5) is retained even at the highest ligand concentration investigated in this work ($[ISA]_{tot}$ = 0.1 M). The decrease in sorption can be explained by the formation of ternary complexes (Ca-)Nb-ISA, as proposed in previous studies with Pu(IV) [34] and Th(IV) [69]. The order of addition of the

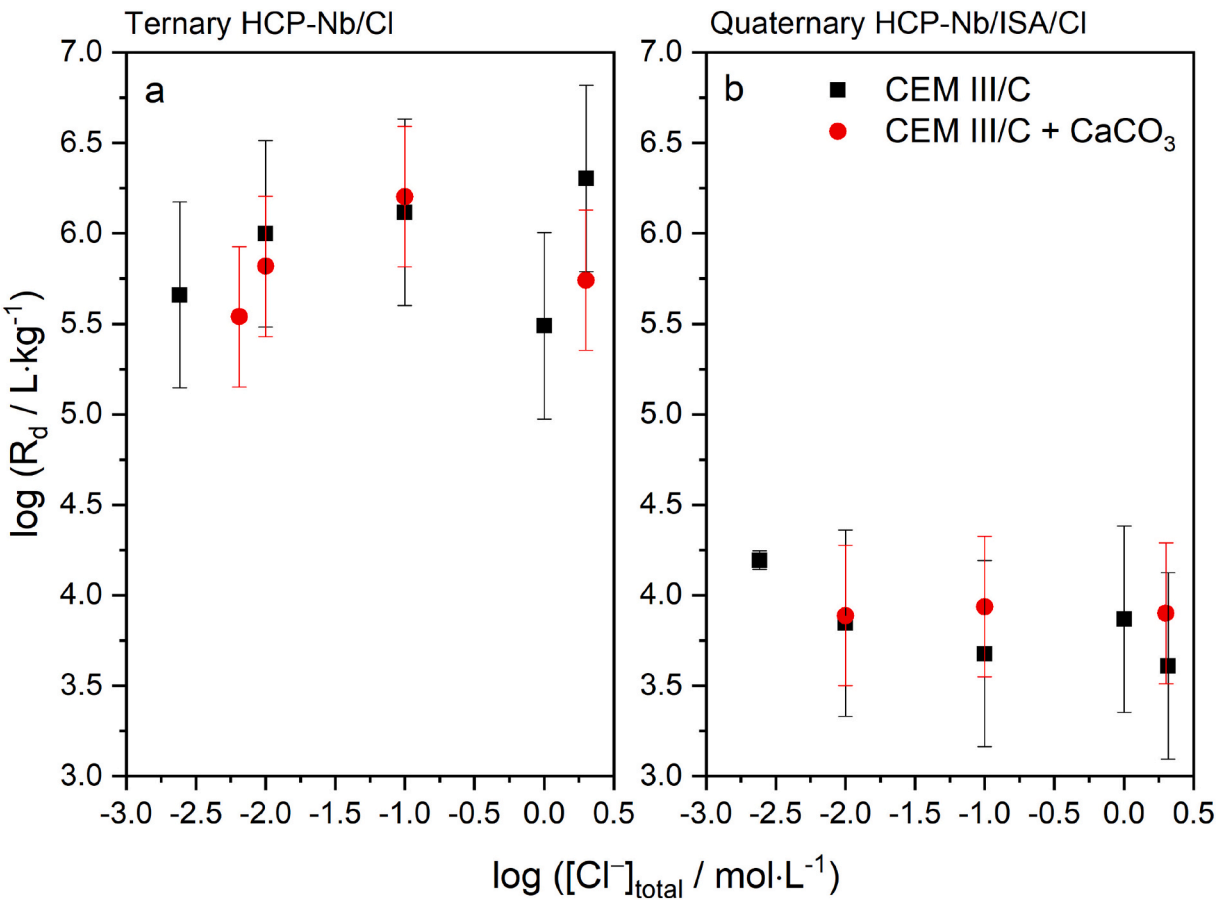

Fig. 5. Impact of Cl^- on the distribution coefficients (R_d) of Nb(V) in HCP (CEM III/C and CEM III/C) in the absence (ternary HCP-Nb/Cl system, left figure a) and presence (quaternary HCP-Nb/ISA/Cl system, right figure b) of ISA. The concentration of ISA in the quaternary system was kept constant at $[ISA]_{tot}$ 0.032 M. Experiments were conducted at S:L 0.5 $g{\cdot}L^{-1}$ and 1.0 $g{\cdot}L^{-1}$ for ternary and quaternary systems, respectively. Experimental details are summarized in Table 1 ("HCP-Nb/Cl" and "HCP-Nb/ISA/Cl"). All data points and corresponding uncertainties are provided in Table SI-5 in Supporting Information.

individual components was found to have an impact on uptake process. The sequence (Nb + cement) + ISA resulted in greater R_d values than (Nb + ISA) + cement. By analogy with the long-term sorption experiments performed for the system cement-Pu(IV)-ISA, we conclude that the uptake observed for the sequence (Nb + ISA) + cement is kinetically hindered and does not represent equilibrium conditions. The impact of chloride on the retention of Nb(V) by HCP sorption was negligible in the ternary HCP-Nb/Cl and quaternary HCP-Nb/ISA/Cl systems.

Quantitative sorption data obtained in this work for niobium provide important information to assess the retention of ^{94}Nb in cement-based repositories for L/ILW. Moreover, the mechanistic understanding attained for this system represents a relevant scientific achievement, and contributes to building trust in the safety concept of such repositories.

CRediT authorship contribution statement

Yongheum Jo: Methodology, Investigation, Writing – original draft, Writing – review & editing. **Neşe Çevirim-Papaioannou:** Methodology, Investigation, Writing – review & editing. **Karsten Franke:** Methodology, Writing – review & editing. **Markus Fuss:** Investigation, Writing – review & editing. **Malene Pedersen:** Methodology, Investigation, Writing – review & editing. **Barbara Lothenbach:** Methodology, Investigation, Writing – review & editing. **Benny de Blochouse:** Conceptualization, Project administration, Writing – review & editing. **Marcus Altmaier:** Conceptualization, Project administration, Funding acquisition, Writing – review & editing. **Xavier Gaona:** Conceptualization, Supervision, Project administration, Funding acquisition, Writing – original draft, Writing – review & editing.

Declaration of competing interest

The authors declare that they have no known competing financial interests or personal relationships that could have appeared to influence the work reported in this paper.

Data availability

Data will be made available on request.

Acknowledgements

This work was partly funded by ONDRAF/NIRAS. KIT-INE acknowledges HZDR for support in using cyclotron at Leipzig and providing the irradiated Zr foil used to obtain the active Nb. Frank Geyer, Annika Kaufmann and Melanie Böttle (KIT-INE) are gratefully acknowledged for the ICP–MS/OES measurements and technical support. We thank Thomas Sittel for the NMR characterization of ISA stock solutions.

References

[1] J.P. Collier, H.W. Song, J.C. Phillips, J.K. Tien, The effect of varying Al, Ti, and Nb content on the phase-stability of Inconel-718, Metall. Trans. A. 19 (1988) 1657–1666.

[2] L. Wang, E. Martens, D. Jacques, P.D. Canniere, J. Berry, D. Mallants, Review of Sorption Values for the Cementitious near Field of a Near Surface Radioactive Waste Disposal Facility, Project near Surface Disposal of Category a Waste at Dessel (NIROND-TR Report 2008-23E, NIRAS-MP5–03 DATA-LT(NF), V1), Brussels, Belgium, 2009.

[3] A.G. Espartero, J.A. Suarez, M. Rodriguez, Determination of Nb-93m and Nb-94m in medium and low level radioactive wastes, Appl. Radiat. Isot. 49 (1998) 1277–1282.

[4] J.P. Adams, M.L. Carboneau, National Low-Level Waste Management Program Radionuclide Report Series, Volume: 11 Niobium-94 (DOE/LLW-127), Idaho National Engineering Laboratory, Idaho, United States, 1995.

[5] ONDRAF/NIRAS, Hoofdstuk 14 - Veiligheidsevaluatie - Langetermijnveiligheid - Veiligheidsrapport voor de oppervlaktebergingsinrichting van categorie A-afval te Dessel. Category A (Technical Report NIROND-TR 2011-14 V3), Brussels, Belgium, 2019.

[6] D. Jacques, Q.T. Phung, J. Perko, S.C. Seetharam, N. Maes, S. Liu, L. Yu, B. Rogiers, E. Laloy, Towards a scientific-based assessment of long-term durability and performance of cementitious materials for radioactive waste conditioning and disposal, J. Nucl. Mater. 557 (2021), 153201.

[7] M. Altmaier, B. Lothenbach, V. Metz, E. Wieland, Preface / special issue “geochemistry research for cement-based materials in nuclear waste disposal applications”, Appl. Geochem. 123 (2020) 104701.

[8] L. Duro, M. Altmaier, E. Holt, U. Mäder, F. Claret, B. Grambow, A. Idiart, A. Valls, V. Montoya, Contribution of the results of the CEBAMA project to decrease uncertainties in the Safety Case and Performance Assessment of radioactive waste repositories, Appl. Geochem. 112 (2020), 104479.

[9] E. Wieland, L. Van Loon, Cementitious Near-field Sorption Data Base for Performance Assessment of an ILW Repository in Opalinus Clay (Technical Report 03–06), Paul Scherrer Institut, Villigen, Switzerland, 2003.

[10] M. Ochs, M. Dirk, L. Wang, Radionuclide and Metal Sorption on Cement and Concrete, Springer, Switzerland, 2016.

[11] U.R. Berner, Evolution of porewater chemistry during degrardation of cement in a radioactive waste repository environment, Waste Manag. 12 (1992) 201–219.

[12] S. Gaboreau, S. Grangeon, F. Claret, D. Ihiawakrim, O. Ersen, V. Montouillout, N. Maubec, C. Roosz, P. Henocq, C. Carteret, Hydration properties and interlayer organization in synthetic C-S-H, Langmuir 36 (2020) 9449–9464.

[13] B. Lothenbach, A. Nonat, Calcium silicate hydrates: solid and liquid phase composition, Cem. Concr. Res. 78 (2015) 57–70.

[14] K. Vercammen, M.A. Glaus, L.R. Van Loon, Complexation of Th(IV) and Eu(III) by alpha-isosaccharinic acid under alkaline conditions, Radiochim. Acta 89 (2001) 393–401.

[15] J. Tits, E. Wieland, M.H. Bradbury, The effect of isosaccharinic acid and gluconic acid on the retention of Eu(III), Am(III) and Th(IV) by calcite, Appl. Geochem. 20 (2005) 2082–2096.

[16] D. Rai, M. Yui, D.A. Moore, L. Rao, Thermodynamic model for ThO2(am) solubility in Isosaccharinate solutions, J. Solut. Chem. 38 (2009) 1573.

[17] A.D. Moreton, N.J. Pilkington, C.J. Tweed, Thermodynamic Modeling of the Effect of Hydrocarboxylic Acids on the Solubility of Plutonium at High pH, Nuclear Industry Radioactive Waste Executive (Nirex), UK, 2000.

[18] A. Tasi, X. Gaona, D. Fellhauer, M. Böttle, J. Rothe, K. Dardenne, R. Polly, M. Grivé, E. Colàs, J. Bruno, K. Källström, M. Altmaier, H. Geckeis, Thermodynamic description of the plutonium – α-d-isosaccharinic acid system I: solubility, complexation and redox behavior, Appl. Geochem. 98 (2018) 247–264.

[19] A. Tasi, X. Gaona, D. Fellhauer, M. Böttle, J. Rothe, K. Dardenne, R. Polly, M. Grivé, E. Colàs, J. Bruno, K. Källstrom, M. Altmaier, H. Geckeis, Thermodynamic description of the plutonium – α–d–isosaccharinic acid system ii: formation of quaternary Ca(II)–Pu(IV)–OH–ISA complexes, Appl. Geochem. 98 (2018) 351–366.

[20] T. Kobayashi, T. Teshima, T. Sasaki, A. Kitamura, Thermodynamic model for Zr solubility in the presence of gluconic acid and isosaccharinic acid, J. Nucl. Sci. Technol. 54 (2017) 233–241.

[21] M.R. González-Siso, X. Gaona, L. Duro, M. Altmaier, J. Bruno, Thermodynamic model of Ni(II) solubility, hydrolysis and complex formation with ISA, Radiochim. Acta 106 (2018) 31–45.

[22] E. Wieland, Sorption Data Base for the Cementitious near Field of L/ILW and ILW Repositories for Provisional Safety Analyses for SGT-E2 (Nagra Technical Report 14-08), Paul Scherrer Institut, Villigen, Switzerland, 2014.

[23] J. Tits, G. Geipel, N. Macé, M. Eilzer, E. Wieland, Determination of uranium(VI) sorbed species in calcium silicate hydrate phases: a laser-induced luminescence spectroscopy and batch sorption study, J. Colloid Interface Sci. 359 (2011) 248–256.

[24] V. Häußler, S. Amayri, A. Beck, T. Platte, T.A. Stern, T. Vitova, T. Reich, Uptake of actinides by calcium silicate hydrate (C-S-H) phases, Appl. Geochem. 98 (2018) 426–434.

[25] M.L. Schlegel, I. Pointeau, N. Coreau, P. Reiller, Mechanism of europium retention by calcium silicate hydrates: an EXAFS study, Environ. Sci. Technol. 38 (2004) 4423–4431.

[26] T. Missana, M. García-Gutiérrez, U. Alonso, O. Almendros-Ginestá, Nickel retention by calcium silicate hydrate phases: evaluation of the role of the Ca/Si ratio on adsorption and precipitation processes, Appl. Geochem. 137 (2022), 105197.

[27] M. Isaacs, S. Lange, G. Deissmann, D. Bosbach, A.E. Milodowski, D. Read, Retention of technetium-99 by grout and backfill cements: implications for the safe disposal of radioactive waste, Appl. Geochem. 116 (2020), 104580.

[28] J.J. Pilkington, N.S. Stone, The Solubility and Sorption of Nickel and Niobium Under High pH Conditions NSS/R186, 1990.

[29] S. Baker, R. McCrohon, P. Oliver, N.J. Pilkington, The sorption of niobium, tin, iodine and chlorine onto nirex reference vault backfill, Mater. Res. Soc. Symp. Proc. 333 (1994) 719–724.

[30] I. Pointeau, C. Landesman, N. Coreau, N. Moisan, P. Reiller, Etude de la retention chimique des radionucleides Cs(I), Am(III), Zr(IV), Pu(IV), Nb(V), U(VI), Tc(IV) par les matériaux cimentaires degradés, (CEA/DEN/SAC Report RT DPC/SECR 03-037), 2004.

[31] Y. Tachi, T. Suyama, M. Mihara, Data Acquisition for Radionuclide Sorption on Barrier Materials for Performance Assesement of Geological Disposal of TRU Wastes (JAEA-Data/Code 2019–021), Japan Atomic Energy Agency, Ibaraki-ken, Japan, 2020.

[32] Y. Jo, K. Garbev, N. Cevirim-Papaioannou, O.D. Blanco, B. de Blochouse, M. Altmaier, X. Gaona, Solubility of niobium(V) in cementitious systems relevant for nuclear waste disposal: characterization of the solubility-controlling solid phases, J. Hazard. Mater. 129810 (2022).

[33] N. Çevirim-Papaioannou, Y. Jo, K. Franke, M. Fuss, B. de Blochouse, M. Altmaier, X. Gaona, Uptake of niobium by cement systems relevant for nuclear waste disposal: impact of ISA and chloride, Cem. Concr. Res. 153 (2022), 106690.

[34] A. Tasi, X. Gaona, T. Rabung, D. Fellhauer, J. Rothe, K. Dardenne, J. Lutzenkirchen, M. Grive, E. Colas, J. Bruno, K. Kallstrom, M. Altmaier, H. Geckeis, Plutonium retention in the isosaccharinate - cement system, Appl. Geochem. 126 (2021).

[35] ONDRAF/NIRAS, Hoofdstuk 5 - Kennis van de fenomenologie van de kunstmatige barrières in hun omgeving - Veiligheidsrapport voor de oppervlaktebergingsinrichting van categorie A-afval te Dessel (Technical Report NIROND-TR 2011-05 V3), Brussels, Belgium, 2019.

[36] S. Busse, J. Brockmann, F. Rosch, Radiochemical separation of no-carrier-added radioniobium from zirconium targets for application of Nb-90-labelled compounds, Radiochim. Acta 90 (2002) 411–415.

[37] V. Radchenko, D.V. Filosofov, O.K. Bochko, N.A. Lebedev, A.V. Rakhimov, H. Hauser, M. Eisenhut, N.V. Aksenov, G.A. Bozhikov, B. Ponsard, F. Roesch, Separation of Nb-90 from zirconium target for application in immuno-PET, Radiochim. Acta 102 (2014) 433–442.

[38] P. Longuet, L. Burglen, A. Zelwer, La phase liquide du ciment hydraté, Rev. Mater. Constr. 676 (1973) 35–41.

[39] B. Lothenbach, F. Winnefeld, Thermodynamic modelling of the hydration of Portland cement, Cem. Concr. Res. 36 (2006) 209–226.

[40] B. Traynor, H. Uvegi, E. Olivetti, B. Lothenbach, R.J. Myers, Methodology for pH measurement in high alkali cementitious systems, Cem. Concr. Res. 135 (2020), 106122.

[41] R. Snellings, A. Salze, K.L. Scrivener, Use of X-ray diffraction to quantify amorphous supplementary cementitious materials in anhydrous and hydrated blended cements, Cem. Concr. Res. 64 (2014) 89–98.

[42] D. Jansen, F. Götz-Neunhoeffer, C. Stabler, J. Neubauer, A remastered external standard method applied to the quantification of early OPC hydration, Cem. Concr. Res. 41 (2011) 602–608.

[43] B. Lothenbach, P. Durdziński, K. De Weerdt, Thermogravimetric analysis, in: K. Scrivener, R. Snellings, B. Lothenbach (Eds.), A Practical Guide to Microstructural Analysis of Cementitious Materials, CRC Press, Boca Raton (FL, USA), London (UK) and New York (NY, USA), 2016, pp. 177–211.

[44] R. Snellings, X-ray powder diffraction applied to cement, in: K. Scrivener, R. Snellings, B. Lothenbach (Eds.), A Practical Guide to Microstructural Analysis of Cementitious Materials, CRC Press, Boca Raton (FL, USA), London (UK) and New York (NY, USA), 2016, pp. 107–176.

[45] R.T. Downs, D.C. Palmer, The pressure behavior of alpha-cristobalite, Am. Mineral. 79 (1994) 9–14.

[46] N.W. Thibault, Morphological and structural crystallography and optical properties of silicon carbide (SiC) - part II structural crystallography and optical properties, Am. Mineral. 29 (1944) 327–362.

[47] T. Runcevski, R.E. Dinnebier, O.V. Magdysyuk, H. Pollmann, Crystal structures of calcium hemicarboaluminate and carbonated calcium hemicarboaluminate from synchrotron powder diffraction data, Acta. Crystallogr. B. Struct. Sci. 68 (2012) 493–500.

[48] JCPDS, Powder Diffraction Files, Joint Committee on Powder Diffraction Standards, Swarthmore, USA, 2001.

[49] E. Wieland, J. Tits, A. Ulrich, M.H. Bradbury, Experimental evidence for solubility limitation of the aqueous Ni(II) concentration and isotopic exchange of ^{63}Ni in cementitious systems, Radiochim. Acta 94 (2006) 29–36.

[50] J. Tits, E. Wieland, C.J. Müller, C. Landesman, M.H. Bradbury, Strontium binding by calcium silicate hydrates, J. Colloid Interface Sci. 300 (2006) 78–87.

[51] J. Tits, K. Iijima, E. Wieland, G. Kamei, The uptake of radium by calcium silicate hydrates and hardened cement paste, Radiochim. Acta 94 (2006) 637–643.

[52] N. Çevirim-Papaioannou, S. Han, I. Androniuk, W. Um, M. Altmaier, X. Gaona, Uptake of Be(II) by cement in degradation stage I: wet-chemistry and molecular dynamics studies, Minerals 11 (2021) 1149.

[53] I. Bonhoure, E. Wieland, A.M. Scheidegger, M. Ochs, D. Kunz, EXAFS study of Sn (IV) immobilization by hardened cement paste and calcium silicate hydrates, Environ. Sci. Technol. 37 (2003) 2184–2191.

[54] C.T.M. Ochs, Development of Models and Datasets for Radionuclide Retention by Cementitious Materials, ANDRA, 2006.

[55] X. Gaona, R. Dähn, J. Tits, A.C. Scheinost, E. Wieland, Uptake of Np(IV) by C–S–H phases and cement paste: an EXAFS study, Environ. Sci. Technol. 45 (2011) 8765–8771.
[56] W. Hummel, G. Anderegg, L. Rao, I. Puigdomenech, O. Tochiyama, Chemical Thermodynamics of Compounds and Complexes of U, Np, Pu, Am, Tc, Se, Ni and Zr with Selected Organic Ligands (Chemical Thermodynamics 9), Elsevier Science Publishers B.V., Amsterdam, Netherlands, 2005.
[57] X. Gaona, V. Montoya, E. Colas, M. Grive, L. Duro, Review of the complexation of tetravalent actinides by ISA and gluconate under alkaline to hyperalkaline conditions, J. Contam. Hydrol. 102 (2008) 217–227.
[58] D. Rai, A. Kitamura, Thermodynamic equilibrium constants for important isosaccharinate reactions: a review, J. Chem. Thermodyn. 114 (2017) 135–143.
[59] I. Pointeau, N. Coreau, P.E. Reiller, Uptake of anionic radionuclides onto degraded cement pastes and competing effect of organic ligands, Radiochim. Acta 96 (2008) 367–374.
[60] D. García, P. Henocq, O. Riba, M. López-García, B. Madé, J.-C. Robinet, Adsorption behaviour of isosaccharinic acid onto cementitious materials, Appl. Geochem. 118 (2020), 104625.
[61] Y. Jo, I. Androniuk, N. Çevirim-Papaioannou, B. de Blochouse, M. Altmaier, X. Gaona, Uptake of chloride and iso-saccharinic acid by cement: sorption and molecular dynamics studies on HCP (CEM I) and C-S-H phases, Cem. Concr. Res. 157 (2022), 106831.
[62] N. Çevirim-Papaioannou, I. Androniuk, S. Han, N.A. Mouheb, S. Gaboreau, W. Um, X. Gaona, M. Altmaier, Sorption of beryllium in cementitious systems relevant for nuclear waste disposal: quantitative description and mechanistic understanding, Chemosphere 282 (2021), 131094.
[63] I. Androniuk, A.G. Kalinichev, Molecular dynamics simulation of the interaction of uranium (VI) with the C–S–H phase of cement in the presence of gluconate, Appl. Geochem. 113 (2020), 104496.
[64] W. Hummel, G. Anderegg, L. Rao, I. Puigdomenech, O. Tochiyama, Chemical Thermodynamics of Compounds and Complexes of U, Np, Pu, Am, Tc, Se, Ni and Zr with Selected Organic Ligands (Chemical Thermodynamics 9), OECD Nuclear Energy Agency, Issy-les-Moulineaux, France, Paris, 2020.
[65] P. Henocq, A sorption model for alkalis in cement-based materials – correlations with solubility and electrokinetic properties, Phys. Chem. Earth: A/B/C 99 (2017) 184–193.
[66] E. L'Hôpital, B. Lothenbach, K. Scrivener, D.A. Kulik, Alkali uptake in calcium alumina silicate hydrate (C-A-S-H), Cem. Concr. Res. 85 (2016) 122–136.
[67] G.D. Miron, D.A. Kulik, Y. Yan, J. Tits, B. Lothenbach, Extensions of CASH+ thermodynamic solid solution model for the uptake of alkali metals and alkaline earth metals in C-S-H, Cem. Concr. Res. 152 (2022), 106667.
[68] M. Balonis, B. Lothenbach, G. Le Saout, F.P. Glasser, Impact of chloride on the mineralogy of hydrated Portland cement systems, Cem. Concr. Res. 40 (2010) 1009–1022.
[69] E. Wieland, J. Tits, J.P. Dobler, P. Spieler, The effect of alpha-isosaccharinic acid on the stability of and Th(IV) uptake by hardened cement paste, Radiochim. Acta 90 (2002) 683–688.